Evaluation of Structural Integrity of Laser Formed Steel Sheets for Possible Load Bearing Applications

S.A. AKINLABI[1]* AND M. SHUKLA[2]

[1]*Department of Mechanical Engineering Science, University of Johannesburg, Auckland Park Kingsway Campus, Johannesburg, 2006, South Africa.*
[2] *Department of Mechanical Engineering, MNNIT, Allahabad, UP, 211004, India & University of Johannesburg, Doornfontein, South Africa.*

*Corresponding author: Phone: +27783160281; Fax: +27 559 2137; E-mail: stephenakinlabi@gmail.com

ABSTRACT

Steel is a well-known material for various manufacturing applications because of its unique properties such as great formability and durability, good tensile and yield strength and good thermal conductivity. This paper reports on the evaluation of the structural integrity of laser formed steel sheets for possible load carrying applications. The tensile tests conducted revealed 46% elongation while the yield strength of the laser formed components were enhanced with about 18%. Furthermore, elongated grain structures were observed in the micrographs of the three components formed at the maximum parameter setting. It was revealed that this elongation varied indirectly to the applied line energy. The measured grain sizes further showed that the components formed at the optimized maximum process parameter window were characterized by smaller grain structures with about 60% of the grain sizes of the parent material. A progressive increase in the micro Vickers hardness of about 40% was also observed in the three laser formed components in comparison to the parent material. The analysis of the residual stresses conducted in this study revealed that the changes in the residual stresses are a function of the process condition to which the samples were subjected. In the case of the parent material, the residual

stresses across the three measured points were compressive. Similarly, the observed differences in the tensile stresses between the three samples formed at the different parameters can be attributed to the effect of the flow stress, the temperature and the cooling rate. The consistently high value of the stress at a particular point designated as point number two can be attributed to the highest temperature recorded at this point, because this is the point where the whole process cycle ends having a high energy density. Looking closely at the stress values captured at the three points, theoretically point two is believed to be the point of maximum deformation; hence, the maximum strain results. At low scan velocity and low temperature, the flow stress associated is high. Therefore, the stress is higher than those at higher velocity. But on the other hand, at high temperatures, the associated flow stress becomes low. It can be summarized that the material characterization and the evaluations conducted on the formed samples revealed the inherent structural integrities.

Keywords**:** structural integrity, laser forming, microstructural evolution, residual stresses

1. INTRODUCTION

Generally, structural integrity involves the conditions affecting strength, corrosion and wear life of mechanical constructions. Hence, study into structural integrity may demand the estimation of mechanical, thermical and chemical stresses that affect the structures and dimensioning for all manufacturer failure such as fracture, wear, fatigue and corrosion etc. In more specific terms, Structural Integrity has been defined as the science and technology of the margin between safety and disaster. Furthermore, another notable expert also reported in a paper titled “Engineering Materialism and structural integrity” that most frontiers of structural integrity have been primarily financial, involving the desire of manufacturers and investors to maximize return on investment, the desire of insurers to have a pre-defined risk, and the possibility of litigation in

event of failure [1]. Until early 19th century, the design engineers relied on using large safety factors (the ratio of the yield strength to the applied stress) in order to overcome the uncertainty associated with the actual strength of various components and structures due to inevitable and undetectable internal defects, this often leads to catastrophic failure of the components. Consequently, the cost of the failure is always very huge for many operators and companies to cope with. These imply therefore, that the integrity of critical facility is considered to be very important for effective and smooth running [2]-[4] when in use. In view of this, Motarjemi and Shirzadi [2] considered the assessment of the structural integrity of a component as an approach to establish whether the structure is fit to withstand the intended service condition safely and reliable throughout its predicted lifetime. Structural integrity was further defined as the capability of a structure to carry out the operation for which it has been designed [5]. The efficient and safe designs of structures such as automotive vehicles, offshore platforms, pressure vessels or process equipment are vital to their continued profitable operation. Therefore, structural integrity measurement is considered to be fundamental to safe and economic operation of manufacturing and production plants, equipment and systems [2].

The measurement of structural integrity of a material can be therefore be based on the knowledge of the loads exerted on the structure, together with an understanding of the local stress environment and the behaviour of the materials used. It was reported that most structures are subject to through-life degradation due to environmental and operating conditions that promote progressive damage mechanisms, such as residual stress, corrosion, or fatigue cracking [2]. Most of the operating conditions directly or indirectly influence the properties (chemical, mechanical) of the component but only within allowable limit for an effective useful life of the component.

Metal forming process among other manufacturing process such as casting, machining, joining, laser sintering, electronic beam melting etc. are considered as manufacturing processes that uniquely change the property of material during the process of converting the stock or raw materials into finished or semi-finished product for different application purposes in domestic and industrial sector. The changes in the property of a formed component or part result from the plastic modification of the solid part. During this process both mass and material cohesion are maintained. Metal forming applications have been successful in many industrial applications such as in automotive industry, aerospace, ship building and other construction applications [5]-[6].

Steel is one of the most desirable metals for most industrial application such as in construction, automotive, shipbuilding, pipeline, mining, heavy equipment, offshore construction, energy and aerospace etc. because of its unique properties such as high strength, heat treatable, toughness, weldability, durability, ductility and stability of mechanical and chemical properties at high temperature [6]. In addition, according to Terrence Bell [7] about 75% of the weight of typical house hold appliances comes from steel. Steel is found in appliances like fridges, washing machines, oven, microwaves, sinks, cutlery etc. However, steel is in abundance and relatively affordable, but it is susceptible to easy corrosion, low fire resistance and buckling and high deformation [8].

Forming has traditionally been the manufacturing process for shaping metallic samples by using dies and presses with external force. Laser Forming (LF), on the other hand, is a non-contact process, and one of the new processes developed for shaping metallic samples without the use of applied force to the sample [9]. In the process, the sheet metals get deformed due to thermal stresses induced by a controlled defocused laser beam scanned over the surface instead of

external mechanical forces [10]. Furthermore, Laser Forming is known to be a novel technique employed to deform plates and sheet metals such as different grades of steels, light alloys of aluminium, magnesium and titanium etc. with a uniqueness of high thermal expansion coefficient. This technique has immense applications in shipbuilding, automotive and aerospace industries. During the laser beam forming process deformation is induced by the process of scanning the laser beam across the surface of the material [11].

Since its invention in the 1980s [6], LBF forming has been successfully applied to a high variety of sheet metal components from both ferrous and non-ferrous metals. Almost 90% of steel manufactured all over the world is carbon steel. These materials are widely used in low strength manufacturing, forming and welding applications. Mechanical properties of steels are strongly linked to the microstructure obtained after a heat treatment process [12][13].

Consequently, temperature gradients are developed through the material thickness inducing stresses as a result of the different thermal expansion of the adjacent layers in the material. It requires no tools and external forces, the process offer great flexibility with other applications and it is easier to incorporate laser beam forming into manufacturing systems. Elimination of springback phenomenon is a major advantage over mechanical forming process [14-[15]. Following the temperature fields developed from the laser scan, Vollertsen proposed three different mechanisms to explain the phenomenon behind metal forming process [16]. They are temperature gradient mechanism (TGM), buckling mechanism (BM), and upsetting mechanism (UP). The principal mechanism activated during laser beam forming process is strongly dependent on the process parameters such as found in the energy parameters, geometric parameters and material parameters. The TGM is based on the difference between rapid laser surface heating and slow conduction of heat from the irradiated point into the bulk. It is

considered principal deformation mechanism when the beam diameter impinging on the material surface is of the same dimension to the material thickness. During the process, a steep temperature gradient is developed through the material thickness, thus result is different thermal expansion.

It is known that laser forming has some significance to industries that have previously relied on dies and presses for forming processes during manufacturing, because of the overwhelming merits of the process flexibility, minimum springback, automation, reduction of manufacturing costs and time. Some of these industries include the aerospace, automotive, shipbuilding, construction, and microelectronics industries [3],[17]-[21]. However, the process of manufacturing varies from product to product but more importantly, the quality of the final product is crucial because the reliability and availability of the product becomes a measure of the acceptance and consequently on the investment in the new manufacturing process. Hence, the quality and the integrity of the product is the overall driver of the manufacturing process. In view of this, the interest of many researchers has been attracted to investigating into laser forming process [11],[13],[17]-[18],[22]-[25] and into the structural integrity of manufactured samples [2-4].

The evolved material properties of the formed sample such as the microstructure, strength, fatigue, residual stress, corrosion and wear etc. is a function of the structural integrity of the manufactured material. Hence, quantifying the structural integrity of manufactured samples involves a process for ensuring that the structural composition of the manufactured samples is not destroyed below the acceptable limits [2-3]. In the case of the laser forming process, the plastic deformation of the material is brought about by the thermal stresses induced in the surface of the metal during the rapid laser heating and cooling. This investigation evaluates the structural

integrity of the formed samples through the study of the tensile strength, microstructural evolution, microhardness, the grain size formations and residual stresses.

2. EXPERIMENTAL PROCEDURE

2.1. Laser Forming

The investigation presented is the laser forming of mild steel with a sample size of the rectangular test piece of 3 mm X 200 mm X 50 mm. The standard chemical composition of the parent material is presented in Table 1. The dominant alloying element from the chemical analysis is Manganese (Mn). As such, the steel may be referred to as Manganese micro alloyed steel. This alloy improves the hardness, ductility, the wear resistance, and more importantly, it eliminates the formation of harmful iron sulphides; and increases the strength at high temperatures. This characteristic has made this steel desirable in the manufacturing industry for forming applications. The test samples were cleaned with acetone in order to remove dirt and oil/grease from make the surface of the samples. The experiments were conducted using a 4.4kW Nd: YAG laser system (DY 044;Rofin) in a continuous wave mode, located at the Council for Science and Industrial Research-National Laser Centre (CSIR-NLC), Pretoria, South Africa. The process parameter range employed for the experiment are as follows: Laser Power ranged between 1800-3000 W, Beam Diameter 12-18 mm and the Scan Velocity varied between 0.04 to 0.08 m/min, number of scan tracks per irradiation varied between one and five and Pure argon gas was employed for cooling and avoid oxidation effect at a flow rate of between 5-15l/min. A schematic of the process is shown in Figure 1. The basic component of a laser beam forming system includes the laser source with beam delivery system, fixed table bed, a robot for holding a fibre optic system, cooling system and computer control system. The actual laser forming experimental set-up is shown in Figure 2. This is a customized open mould upon which the

samples were kept for the forming process. The mould provides a very stable platform and permanent position for the samples and also ensures the alignment of the samples in the direction of the laser beam. The choice for an open mould was considered for the experimental set-up in view of the preliminary study, in which both open and cantilevered moulds were employed. It was noted that an open mould provided an opportunity for maximum deformation of the sample during the process, and also enhances the production of multiple formed samples. In addition the open mould approach also help to facilitate the possibility of scanning the samples from either end of the mould. The process parameters considered for this experiment are three sets of parameters, which were the optimized parameter windows in the upper, medium and low band of the process parameters. Both the parent material and the formed components were consequently characterized.

2.2. Tensile test

The tensile samples were produced from the parent materials and tested, in accordance to the ASTM E-8 standard [26]. A servo-hydraulic Instron 8801 tensile testing machine was used to conduct the tests. An extension rate of 5 mm/min and a gauge length of 50 mm were used. The schematic of the sample preparation for the tensile tests is shown in Figure 3 (a) and (b).

2.3. Optical microscopy/SEM analysis

All the specimens for microscopy analysis were taken from specific locations on the sample with the dimension size of 40 X 10 X 3 mm^3 for the steel sheets. The sections of the samples for analysis were taken at 80 mm length, and at about the center position on the width of the sample. The mounted samples were prepared by using a standard metallographic procedure for preparing steel. The polished specimens were etched with the Nital solution (2%) by totally submerging the mounted sample in the solution for 40 seconds; the microstructure was thereafter observed under

the Olympus PMG3 optical microscope and Scanning Electron Microscope (TESCAN). The measurement of the grain sizes of the parent material and the formed specimen were carried out, according to the ASTM E112-96 standard test method for determining average grain size [27]. The measured grain sizes for both the parent material and the formed samples are presented in the chapter on results and discussion.

2.4. Micro Vickers hardness profiling

The Vickers microhardness profiles were measured using the FM-ARS 9000 automatic indenter, according to the ASTM 384 standard [28]. The measurements were made along the cross-section of each sample considered in this test at about the centre of the sample thickness. In particular for the parent material, the three sets of samples were tested with an average micro Vickers harness value while for the laser formed samples, the test was conducted on the treated area and the average micro Vickers hardness values were recorded. A load of 300 g and a dwell time of 15 seconds were employed. The indentations were taken at 0.3 mm intervals, and all the indentations were manually focused and read to ensure that all the measurements were made on the specimen and not on the polyfast. All the measurements were taken in the as-polished condition.

2.5. Residual stresses

Residual stresses are vital to the overall strength and life of critical samples. Most manufacturing processes can develop residual stresses that may be either detrimental or beneficial to the strength and durability of the sample [20]. As such, the residual stress measurements of both the parent material and the formed samples were conducted using the X-ray diffraction technique and a diffractometer (D8 GADDS; BRUKER) was used. The residual stresses were measured at points (1, 2 and 3) as shown in Figure 4 and the residual stress measurement set-up on the

diffractometer is shown in Figure 5. The residual stresses were quantified according to the ASTM E2860 – 12 standard [29].

3. RESULT AND DISCUSSION

3.1. Processing parameters

The optimum process parameters presented in Table 1 were generated from the set of L27 Orthogonal arrayed parameters. The various parameters and their levels are also presented in Table 2. The three optimal ranges were necessary in order to capture the maximum, medium and minimum band of the response of the treated materials.

Laser forming, being a process that employs a defocused laser beam for irradiating the surface of a sample, consequently generates a high surface temperature and large thermal gradients to bring about the deformation of the samples. Hence, the line energy is the ratio of the laser power to the laser scanning speed. It is important to note that a laser line energy threshold must be exceeded in order to initiate permanent deformation under the laser forming process.

3.2. Tensile test

3.2.1 Parent material

The summary of the tensile test results of the parent material is presented in Table 3. The average Ultimate Tensile Strength (UTS) and the Yield Strength (YS) of the three tensile tested samples are presented. The labels T1, T2, and T3 are representative of the three replicate tensile samples machined from the parent material. The schematic of the sample preparation of the tensile samples taken in the transverse direction of the rolling direction is shown in Figure 3b and the tensile specimen is shown in Figure 3a. The tensile behaviour of the replicates of the parent material is shown in Figure 6 with an average of the three samples. However, taking an average of more than three samples for the test may improve the average value of the tensile strength.

The stress-strain curves also demonstrate the ductile nature of the ferritic steel. This unique property makes this grade of steel very suitable for forming applications. The percentage elongation, being a measure of the ductility of the material, was estimated to be an average of 46%.

3.2.2 Laser formed components

It is important to highlight that the rapid heating and cooling of the laser forming process affects the mechanical properties of the formed samples. The investigation of Knupfer and Moore [30] established a relationship between Vickers hardness and the strength of a material. Hence, the yield strength of a processed material was estimated based on the developed empirical relationship presented in Equation 1.

$$YS = 9.81\left[\frac{H}{3}\right](0.1)^n \text{ ----------(1)}$$

Where,

H is the microhardness, and

n is the strain hardening index, which is 0.21 (for steel).

Furthermore, Equation 1 also reveals the existence of a linear relationship between microhardness and Yield Strength. Consequently, the results of the microhardness measurements and the tensile tests showed that the magnitude of hardness, and yield strength are dependent on the mutually interactive influences of the resistance offered to the motion of dislocations, and the plastic deformation capability of the steel sheets. The results of the calculated and the experimental values of the yield strength of the formed samples and the parent material are presented in Table 4.

The results of the calculated values of the yield strength of the laser beam formed samples showed an increase in the yield strength after laser forming, which were in agreement with other published work [31]-[37]. This can be attributed firstly to the cold working of the material induced by the bending strains due to the laser forming. For higher line energies, the increase in hardness at the surface is even more pronounced because in addition to the cold working and recrystallization, small carbon particles have the tendency to dissolve from the pearlite and form around the ferrite grain boundaries at elevated temperatures, thereby resulting in strain hardening of the material.

3.3. Microstructural characterization

A process of rapid heating and cooling cycles as in the case of laser forming, often times cause severe microstructural changes, such as phase transformation or dynamic recrystallization in the generated microstructural zones. The effect of this process would be more significant when multiple laser scans are employed. Hence, the detailed characterization to evaluate the evolved metallurgical properties of the formed sample is hereby presented.

3.3.1 As-received Material

Characterizing the microstructure of the as-received material was conducted in order to compare it with the developed microstructural changes in all the formed samples. The micrograph of the microstructure is shown in Figure 7. It was observed that the dominant lighter pigments were distributed mostly across the grain boundaries.

3.3.2 Laser formed components

The characterized nine samples were formed based on the process parameters presented in Table 1 but a representative set of sample number 22, 23 and 24 is presented in this paper. The

microstructural evolution of the laser formed samples based on the maximum parameters is shown in Figure 8.

3.3.2.1 Maximum parameter setting

This group of formed samples is 22, 23 and 24 according to the process parameters presented in Table 1. The micrographs are shown in Figure 5 (a), (b) and (c) respectively. It was observed in the micrographs for the representative formed samples at maximum parameters that the pearlites were found to be distributed along both the grain boundaries and the elongated ferrites. This can be attributed to the effect of the energy input, resulting in the deformation and recrystallization of the grains. The phenomena behind the laser forming showed that the thermo-mechanical process involves the heating and the cooling phases. In the instance of the heating phase, when the laser beam irradiates the surface of the specimen, the temperature on the surface of the sheets material in the heated region increases rapidly; this does not exceed the melting point of the material. A strong temperature gradient mainly occurs along the direction of the thickness of the specimen. However, as a result of the large thermal expansion and low yield stress on the upper surface layer under the high temperature, the heated region of the material produces compressive plastic deformation, and causes the material to accumulate. Thus, the specimen deformation is increasing. In addition, due to the heat of conduction, the heat energy conducted to the lower surface layer of the sheets is consolidated into the sample and this therefore, makes the temperature within the thickness of the specimen to increase appreciably.

During the cooling phase, after the process is completed, the temperature on the upper surface drops very quickly. The material contracts, so that part of the accumulated material recovers, and the compressive stress decreases. With the continuation of the cooling process, and the heating being conducted, the layers below expand continually and also elongate. Thus, the deformation

away from the laser beam increases. Therefore, the final deformation angle is the result of the combined actions of the thermal deformation process. The resulting bending phenomena can be explained using the bulking mechanism considering that the diameter of the laser beam is larger than the sheets thickness. In view of this, the microstructural changes in the formed steel are expected due to the effect of heating and cooling during the forming process. Consequently, permanent deformation results from any of the forming mechanism approach and the heat supplied from the laser beam automatically influences the microstructure of the formed steel sheets. In addition, the rate of cooling may also play an important role in the evolving microstructure; even though some researchers have reported that the cooling effect has little or no significant effect on the resultant microstructure of laser formed samples [38]-[41]. At this point, the samples formed at the maximum parameter settings which were produced at a high laser power setting leading to high dissolution of carbon particles present in the steel material would not be the choice for certain industrial applications because the literature, [33],[41] reported that the dissolution of carbon particles occurs at an austenitic temperature, and as such this dissolution may reduce the strength and hardness of the formed sample.

3.4. Micro Vickers hardness profiling

The microhardness values of the as-received material and the three set of formed sample in the three band categories of the parameters are shown in Figure 9.

The profiles showed that the hardness values ranged between the minimum and the maximum values for both the as-received material and the formed samples. This can be attributed to the effect of the manufacturing process on the material, during which there was a rapid heating and cooling that alter and affect the properties of the material. The microhardness profiling for the parent material shows an average value of 94HV. On the other hand, a progressive increase was

observed between the representative formed samples 22, 23 & 24 with average micro Vickers hardness value of 156HV. The increase in the values of the microhardness as observed in the laser formed samples when compared to the parent material was appreciable with a minimum average percentage increase of 47%. The appreciable increase in the micro Vickers hardness values observed in the formed samples over the parent material could be further attributed to the plastic deformation and mechanical work hardening experienced during the process. The results observed correlate with the published results of other researchers in this field [18],[33],[35],[38].

3.5. Residual stress determination

3.5.1 Parent material

The residual stress tensor results measured for points (1, 2 and 3) for the parent material are presented in Table 5. It was observed that all the residual stresses measured in the parent material were found to be compressive in nature. This is expected because the material has not been subjected to the laser forming process, which is believed to influence the structural formation if subjected to laser forming process.

3.5.2 Laser formed components

The summary of stress tensors for the formed component is presented in Table 5. The parameter window was earlier presented in Table 1, with line energy of 60 J/min and five scans per laser track. The stresses developed in all the formed samples are tensile, as presented in Table 5. Hence, at higher temperatures, the stress change caused by the strain rate change is significant. The samples were formed with line energy of 16.36 x 10^3 J/min and five scans per laser track. Looking at the laser formed samples at high parameter window (i.e. formed at a scan velocity of 0.05 m/min, Line Energy (LE) of 60 J/min and the samples of LF – minimum formed at 0.05 m/min, LE of 48 J/m), it was observed that the residual stresses increase, as the LE increases. The LF minimum is the sample with the minimum parameter window; hence, this has the least deformation, bend angle, LE, and microhardness value; while the LF maximum is the sample

with the maximum parameter window hence, the largest deformation that resulted in the maximum bend angle, maximum LE, number of scans and hardness value.

Theoretically point 2 is believed to be the point of maximum deformation; hence, it is the point of maximum strain. The stress values presented in Table 5.18 are in agreement with the earlier published work [40]-[41] that the LE also increases from the LF minimum to a LF maximum; this consequently impacts on the values of σ_{11} of the stresses to be 146.7±48.3 (LF minimum), 90.1±57.9 (LBF medium) and 167.6±49.0 (LF Maximum) respectively. The higher the line energy, the larger the bend angle; and the higher the bend line energy, consequently increases the residual stresses that develop. This was in agreement with the result of Li and Yao [40] on their investigation on laser forming with constant line energy. They found that the residual stresses are lower for samples scanned at higher velocities than at lower velocities.

Similarly, the investigation of Knupfer et al., [30] investigation also confirmed that the heat input associated with higher LE and multiple passes consequently increases the residual strain in the material. The structural transformations occurring in the material induce strains and stresses that alter its stress condition from that of a compressive nature to a tensile condition after the laser forming process.

The iron-carbon diagram, explaining how the microstructure changes with temperature, best describes the microstructural development of an LF. The iron carbon diagram at room temperature showed the presence of ferrite and pearlite. Ferrite, being a fairly soft material can only dissolve a very small amount of carbon (not more than 0.021% at 910^{o}C, and 0.008%) at room temperature. Such a ferrite matrix may contain largely other elements, like Nickel, Cobalt, and Chromium etc. The presence of these elements is the explanation for the increased hardness of a laser beam formed sample, which improves the hardenability and strength.

At elevated temperatures, the formation of austenite begins when steel is heated above its lower critical temperature (710^{o}C), but the structure is fully austenitic above its upper transformation temperature (910^{o}C).

Both the tensile and compressive stresses have their distinctiveness; and the stress values are strongly regulated because different industrial applications would require different permissible stress levels. It is expected that the residual stress value developed in a processed sample should not exceed 80% of the yield strength of the as-received material; this was based on the findings of Schajer's investigation [42]-[43]. With reference to Table 4 showing the calculated yield strength of the samples formed at the three parameter settings, the claim of Schajer was confirmed with the results from this study showing that the residual stress developed during the experimentation at the three parameter settings (minimum, medium and maximum) showed that the values are less than the 80% of the yield strength suggested from Schajer's investigation (55.2%, 34% and 63% for the three parameters respectively). In essence, this range may be regarded as a safe window for the residual stress of a processed material.

4. Conclusion

Characterization of the material properties of a laser formed steel sheets was conducted with the aim of evaluating the structural integrity of the laser formed steel components for possible load bearing applications. The characterization of both the parent material and the formed samples focused on the tensile test, microstructural evaluation, grain size measurements, micro Vickers hardness profiling and residual stress measurements. The experiments were structurally designed through the L27 Orthogonal array but the samples produced with optimized maximum process parameter window were investigated and reported. The tensile tests conducted revealed 46% elongation while the yield strength of the laser formed components increased with about 18% of

the parent material. The measured grain sizes showed that the components formed at the maximum parameter window deformed with smaller grain structures of about 60% of the parent material. Furthermore, a significant increase of 40% was observed in the micro Vickers hardness for the three laser formed component in comparison to the parent material. The high percentage increase is attributed to the high energy density employed in the laser forming process. Even though the percentage increase in the hardness is required for the enhancement of the material after process, it is generally recommended that a maximum of 40% increase in hardness value is recommended for every processed material in order to avoid metallurgical notch. The observed changes in the grain structures with 60% smaller than the parent material, the increased microhardness and the increased yield strength basically indicates the degree of the microstructural evolution of the formed components and measures the structural integrity of the components after the laser forming process. The analysis of the residual stresses conducted in this study revealed that the changes in the residual stresses are a function of the process condition to which the samples were subjected. In the case of the parent material, the residual stresses across the three measured points were compressive. Similarly, the observed differences in the tensile stresses between the three samples formed at the different parameters can be attributed to the effect of the flow stress, the temperature and the cooling rate. The consistently high value of the stress at point two which is located at the center of the sample can be attributed to the highest temperature recorded at this point, because this is the point where the whole process cycle ends correlating to a high energy density.

Acknowledgements

The Rental Pool Programme of National Laser Centre, Council of Scientific and Industrial Research (CSIR), Pretoria, South Africa and the UJ-URC funding supported this work and Mr. Stephen Akinlabi also acknowledges the grant award of the African Laser Centre bursary.

References

[1] Nell M.J. Engineering materialism and Structural Integrity. *Journal of Engineering Design*, **9** (4) (1998), 329-342.

[2] Motarjemi A. and Shirzadi A. (2012). *Structural Integrity Assessment of Engineering Samples*. Retrieved 18th March 2015, from http://www.msm.cam.ac.uk/phasetrans/2006/SI/SI.html

[3] Nash F. (2012). *Structural Integrity Assessment*. Retrieved 25th March 2015, from http://www.fnc.co.uk/Portals/0/downloads/StructuralIntegrity.pdf

[4] TPP (2012). *Yield strength and heat treatment*. Retrieved 18th March 2015, from http://www.tppinfo.com/defect_analysis/yield_strength.html

[5] Grieve D.J. (2009). *Manufacturing processes-Metal forming*, Retrieved 18th February 2015, from http://www.tech.plym.ac.uk/sme/mfrg315/metform1.htm

[6] The free encyclopedia for UK steel construction information (2012). *Steel material properties*. Retrieved 29th April 2015, from http://www.steelconstruction.info/Steel_material_properties

[7] Bell T. (2012). *Steel Applications*. Retrieved 27th April 2015, from http://metals.about.com/od/properties/a/Steel-Applications.htm

[8] Civil Engineering Community (2012). *Advantages and Disadvantages of Steel Structures*. Retrieved 29th February 2015, from http://civilengegy.blogspot.com/2012/02/advantages-and-disadvantages-of-steel.html

[9] Mehdi Z. and Esmaeli Z. Experimental and numerical analysis of bending angle variation and longitudinal distortion in laser forming process. *Scientia Iranica B,* **19** (4) (2012), 1074-1080.

[10] Kuntal M., Pratihar D.K. and Nath A.K. Laser forming of dome shaped surface: Experimental Investigations, Statistical analysis and neural network modeling. *Optics and Lasers in Engineering* **53** (2014), 31-42.

[11] Majumdar, J.D., Nath, A.K. and Manna, I. Studies on laser bending of stainless steel. *Materials Science and Engineering* **A** (385) (2004), 113-122.

[12] Mebarki N., Delagnes D., Lamelse P., Delmas F. and Levaillant C. Relationship between microstructure and mechanical properties of a 5% Cr tempered martensitic tool steel. *Mat. Sci. Eng.* **A**. (387-389) (2004), 171-175.

[13] Majumdar D. and Manna I. Laser material processing. International *Material Reviews* **VOL 56**, (5/6) (2011) 341-388. DOI 10.1179/1743280411Y.0000000003.

[14] Shen H., Shi Y. and Yao Z. Numerical simulation of the laser forming of plates using two simulation scans. *Computational Materials Science* **37** (3)(2006), 239-245.

[15] Yao Z., Shen H., Shi Y. and Hu, J. (2007). Numerical study on laser forming of metal plates with pre-loads. *Computational Materials Science* **40** (1)(2007) 27-32.

[16] Vollertsen F. Mechanisms and models for laser forming. *Laser assisted net shape engineering, in: Proceedings of the LANE (1994), vol. 1*, Meisenbach Bamberg, 345–360.

[17] Akinlabi S. and Akinlabi E. Effect of Process parameters on the laser beam formed Titanium Alloy. *Key Engineering Materials* (622-623) (2014), 1193-1199.

[18] Akinlabi S. and Akinlabi E. Experimental Investigation of Laser beam forming of Titanium and Statistical Analysis of the effects of Parameters on Curvature. *Preceding's of the International MultiConference Engineers and Computer Scientist (IMECS 2013),* Hong Kong 14 -16 March 2013.

[19] Kannatey-Asibu E. *Principle of laser materials processing*. New York: John Wiley & sons, Inc. 2009.

[20] Watkins K.G., Edwardson S.P., Magee J., Dearden G. and French P. Laser forming of aerospace alloys. *The Aerospace Manufacturing technology Conference: Society of Automotive Engineers*. 10-14 September 2001. Washington State Convention & Trade Centre Seattle, Washington, USA. 2001-01-2610.

[21] Walczyk D.F. and Vittal S. Bending of titanium sheets using laser forming. *Journal of Manufacturing Processes*, 2 (4,) (2001), 258-269.

[22] Yang L.J., Tang J., Wang M.L., Wang Y. and Chen Y.B. Surface characteristics of stainless steel after pulsed laser forming. *Applied Surface Science*, **256** (2010), 7018- 7026.

[23] Edwardson S.P., Edwards K., Carey C., Dearden G. and Watkins K.G. Laser forming for ship building applications. *Steel Tech.* **2** (4) (2008).

[24] Namba Y. Laser forming of metals and alloys. *The Laser Advance Material Processing (LAMP 1987)*, 37-44.

[25] Geiger M., Vollertsen F. and Deinzer G. Flexible straightening of car body shells by laser forming. *Sheets Metal and Stamping Symposium, SAE Special Publication* **944** (1993), 37-44.

[26] ASTM International ASTM E3E8M-13a (2013), Standard Tension Testing of Metallic Materials.

[27] ASTM International ASTM E112-96^{e3} (2004), Standard Test mrthods for Determining Average Grain Size.

[28] ASTM International ASTM E384-06 (2006), Standard Test Method for Microindentation Hardness of Materials.

[29] ASTM International ASTM E2860-12 (2012), Standard Test mrthods for Residual Stress Measurement by X-Ray Diffrecation for Bearing Steels.

[30] Knupfer S.M. and Moore A.J. The effect of laser forming on mechanical and metallurgical Properties of low carbon steel and aluminium alloy samples. Journal *of material Science and Engineering*, **527** (16-17), (2010), 437-4359.

[31] McGrath P. An investigation of residual stresses induced by forming processes on the fatigue resistance of automotive wheels. PhD thesis, University of Plymouth. 2001.

[32] Els-Botes A. Material characterizations of laser formed dual phase steel Sample. D.Tech thesis. Nelson Mandela Metropolitan University. 2005.

[33] Thompson C. and Pridham M. Material property changes associated with laser forming of mild steel Sample. *Journals of Materials Processing Technology* **118** (2001), 40-44.

[34] Akinlabi S.A., Marwala T., Akinlabi E.T. and Shukla M. Effect of Scan Velocity on Resulting Curvatures during Laser Beam Bending of AISI 1008 Steel Plate. *Journal of Advanced Materials Research* **299-300** (2011), 1151-1156.

[35] McGrath P.J. and Hughes C.J. Experimental fatigue performance of laser formed Samples. *Optics and Lasers in Engineering* **45** (3) (2007), 423–430.

[36] Akinlabi S.A**.,** Akinlabi E.T. and Shukla M. Effect of Laser Forming on Microstructure and Mechanical Properties of AISI 1008 Steel. ASME Applied Mechanic and Material Conference *(McMat* 2011). May 30- June 2, 2011, Chicago, Illinois, USA.

[37] Akinlabi S.A., Marwala T., Shukla M. and Akinlabi E.T. Laser Forming of 3 mm Steel Plate and the Evolving Properties. *Journal of Academic of Science, Engineering and Technology* 59 (2011), 2279-2283.

[38] Huang F., Jiang Z., Liu X., Lian J. and Chen L. Microstructure and properties of thin wall by laser cladding forming. *Journals of Materials Processing Technology* **209** (2009), 4970-4976.

[39] Shen H. and Yao Z. Study on mechanical properties after laser forming. *Optics and lasers in Engineering* **47** (2009), 111-117.

[40] Li W. and Yao Y.L. Laser forming with constant Line Energy. *International Journal of Advance Manufacturing Technology* **17** (2001), 96-203.

[41] Stefan K., Paradowska A.M., Kirstein O. and Moore A. Investigation of Residual Stress in Laser Forming Steel Plates using Neutron Diffraction. *Material Science Forum* **652** (2010),123-128.

[42] Schajer G.S. Measurement of Non-uniform Residual stresses using the hole-drilling method, Part I- Stress calculation procedures. *Journal of Engineering materials and Technology*, **1** (110) (1998), 335-343.

[43] Schajer G.S. Advances in Hole-Drilling Residual Stress Measurements. *Experimental Mechanic* **50** (2010), 159-168.

List of Tables

TABLE 1
Laser Forming parameter.

Run Order	Optimal Range	P	B	V	N	C	Average Bend Angles	Line Energy (J/m) $x10^3$
22	Maximum	3	2	1	3	1	11.8	60
23		3	2	1	3	2	12.5	
24		3	2	1	3	3	12.7	

TABLE 2
LBF factors and three corresponding levels.

Factors	Name	Units	Levels		
			1	2	3
P	Laser power	W	1800	2400	3000
B	Beam diameter	mm	12	15	18
V	Scan speed	m/min	0.05	0.08	0.11
N	Number of scan		1	3	5
C	Coolant flow rate	l/min	5	10	15

TABLE 3
Tensile test results of the parent material.

					Average
Material Property		T1	T2	T3	(MPa)
Ultimate Tensile strength (UTS)		320.98	324.38	326.90	324.09
Yield Strength (YS)	Upper	282.15	269.48	252.11	267.91
	Lower	243.39	246.69	247.52	245.87
Percentage elongation (%)		46.92	46.04	45.30	46.09

TABLE 4
Summary of calculated and experimental Yield Strength values.

Run order	Optimal Range	Line Energy (J/m) x 10^3	Average Bend angle (^{o})	HV	Estimated YS (MPa)
22	Maximum	60	11.8	155.3	312.32
23			12.5	153.5	309.24
24			12.7	156.6	315.44
PM (Experimental)				94	267.91

TABLE 5
Strsss tensor for both parent material and laser formed component (max parameter).

Measurement points	As-received material (PM)		LBF sample at high parameter window	
	σ_{11}	σ_{22}	σ_{11}	σ_{22}
1	-310.7±27.5	-399.5± 27.5	15.7±41.7	124.1±39.8
2	-299.8± 28.4	-319.6±28.5	167.6±49.0	169.2 ± 52.9
3	-297.0±29.2	- 321.8±29.2	125.8±112.0	102.9±82.7

List of Figures

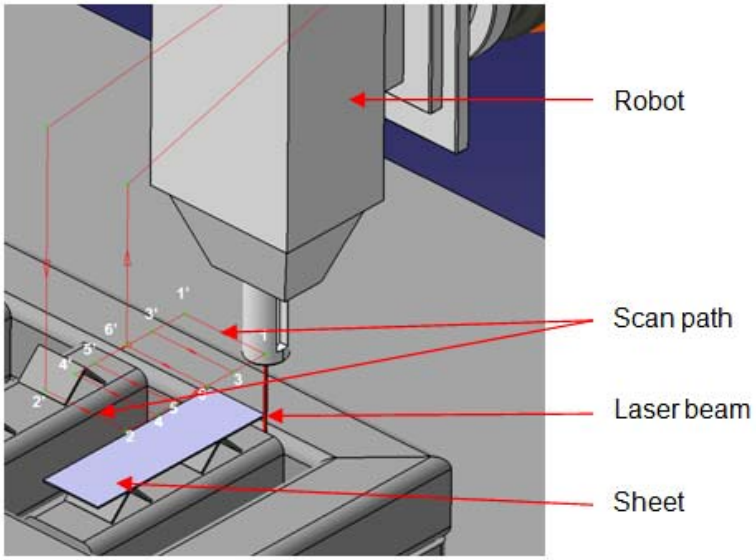

FIGURE 1
Schematic drawing of the Laser Forming Process.

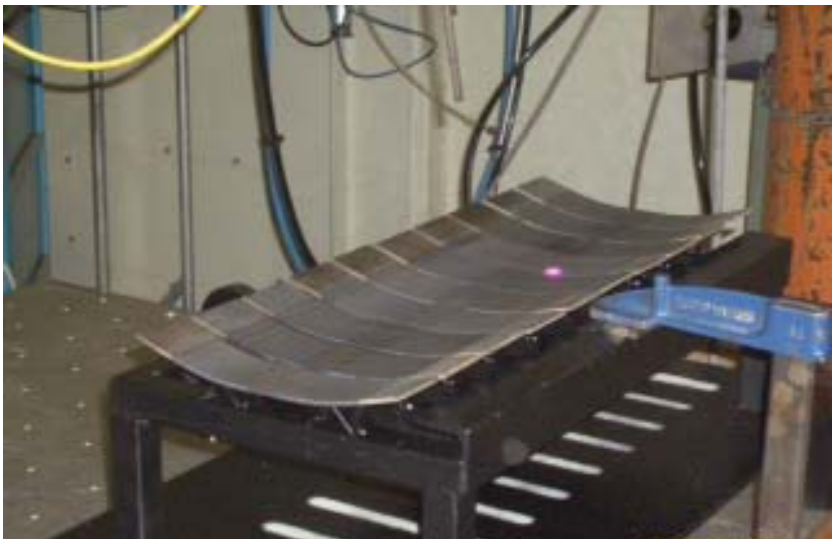

FIGURE 2
Experimental setup of the laser forming process.

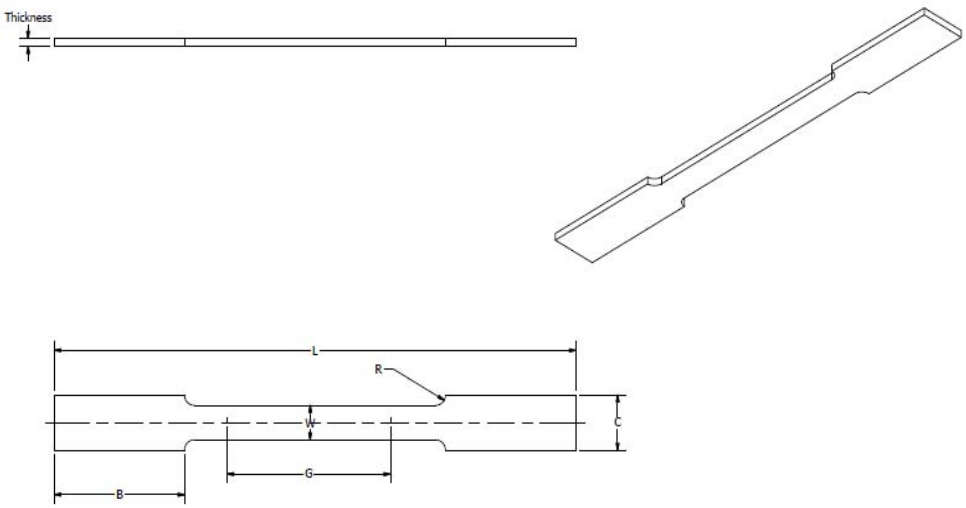

(a)

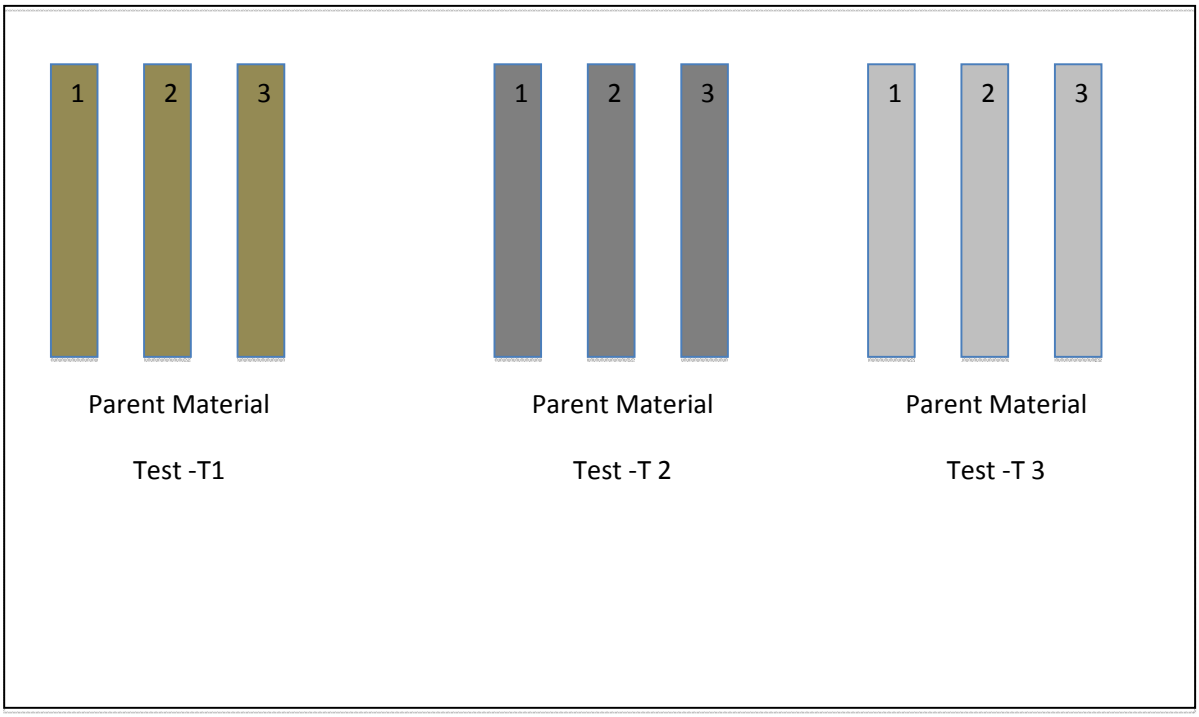

(b)

FIGURE 3

(a) Schematic of Tensile Test sample of parent material.

(b) Schematic of sample preparation for tensile samples taken in transverse direction to the rolling direction.

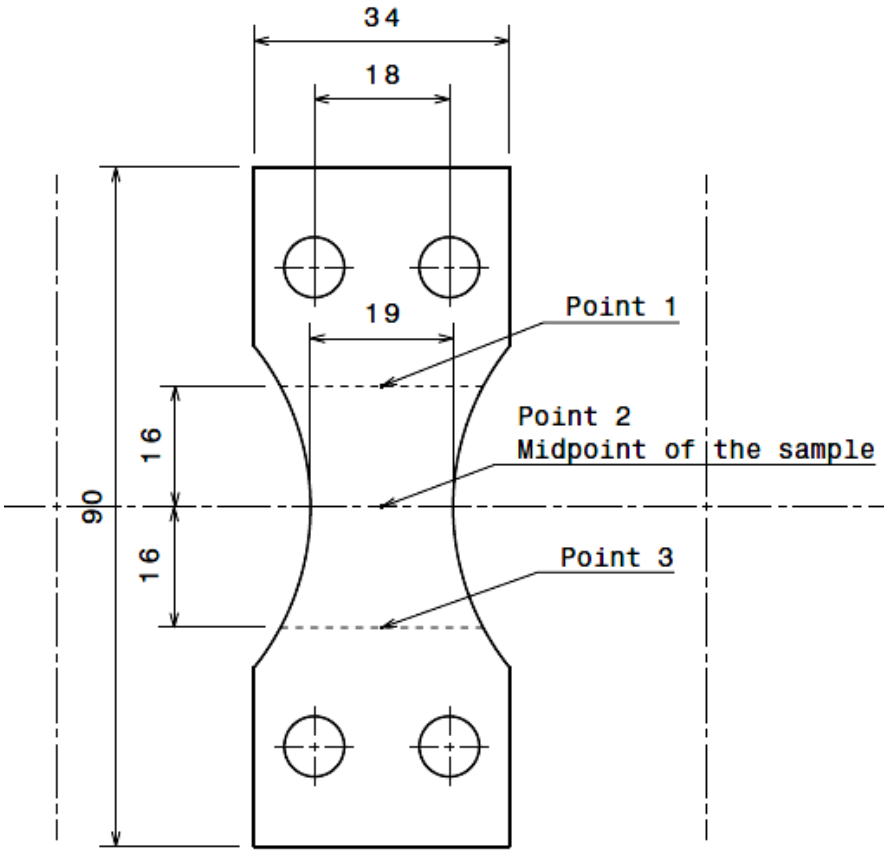

FIGURE 4
Residual stress measurement points.

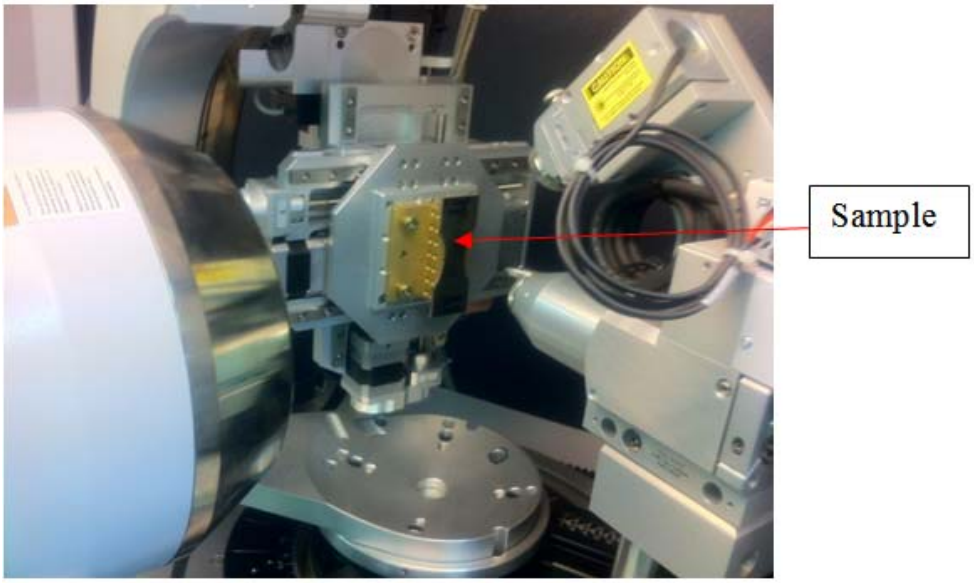

FIGURE 5
Residual stress measurement set-up on the diffractometer

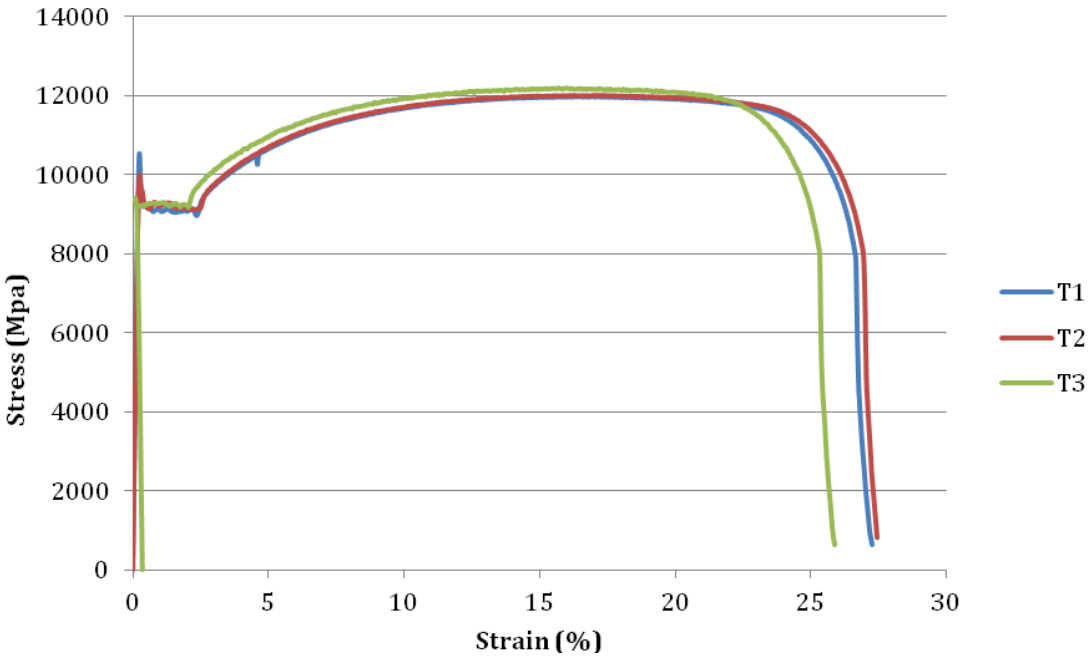

FIGURE 6
Tensile behaviour of the three replicates.

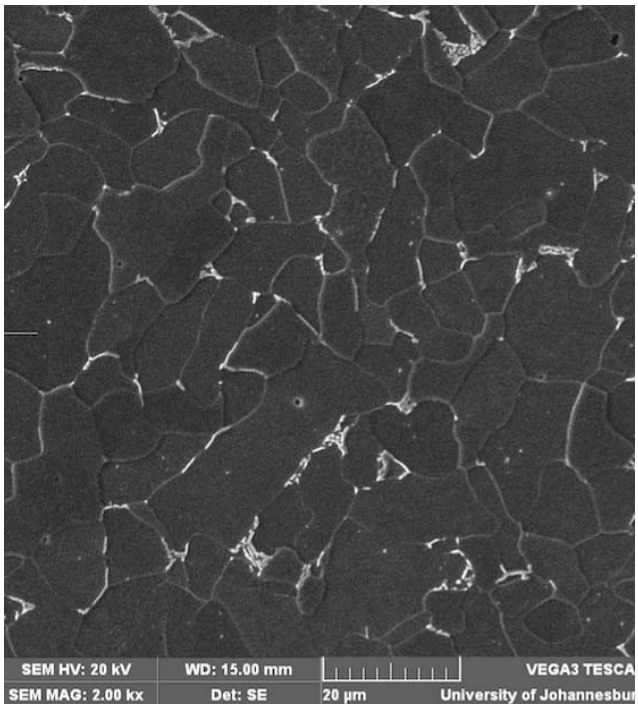

FIGURE 7
SEM Micrograph of the parent material.

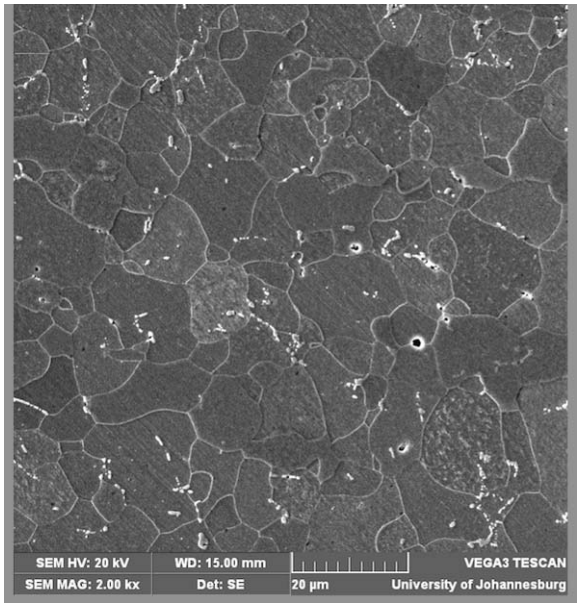

(a)

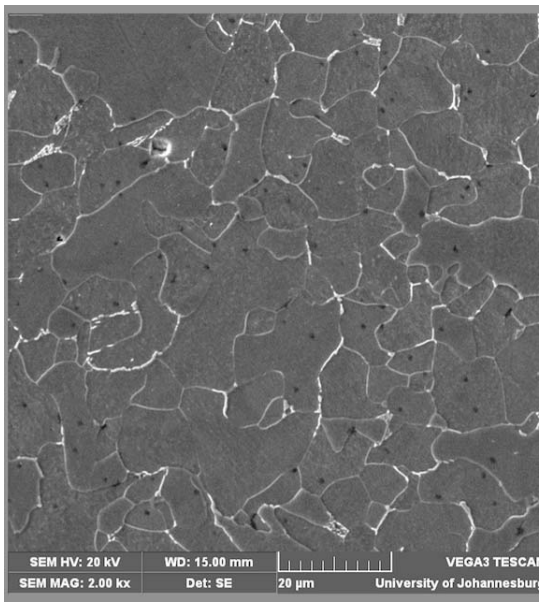

(b)

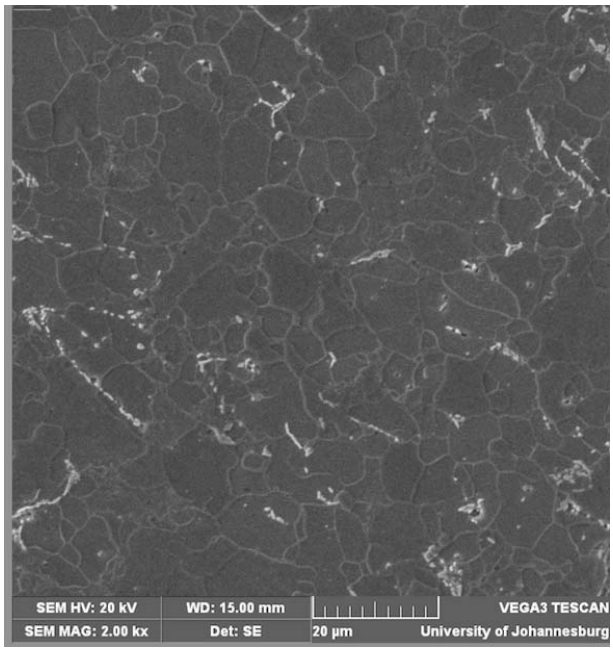

(c)

FIGURE 8
SEM Micrographs of components formed at maximum parameter setting.
(a) Sample 22; (b) Sample 23; (c) Sample 24;

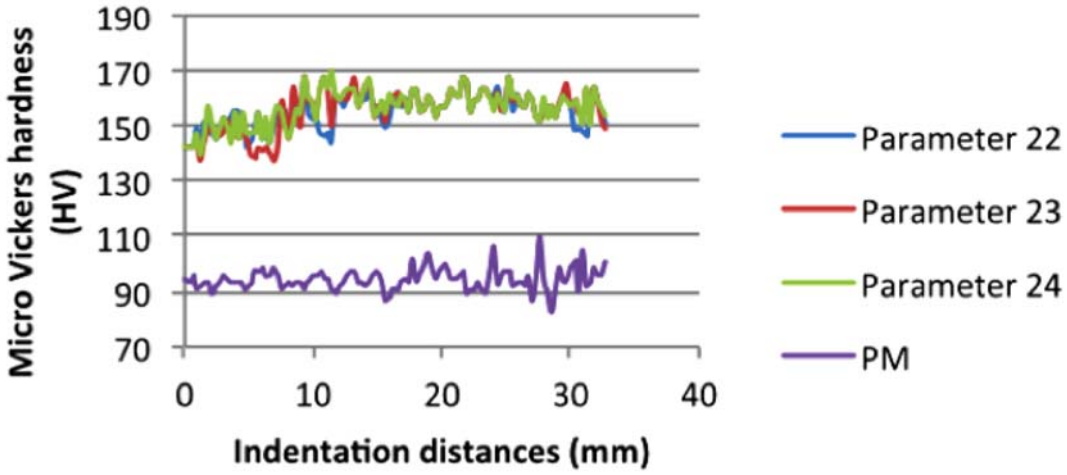

FIGURE 9
Micro Vickers hardness profile for the parent material and the three sets of formed components.

Where, PM is the parent material and 22, 23 and 24 are samples formed at the maximum parameter settings.